CONSTRUCTAL DESIGN OF T-SHAPED HIGH CONDUCTIVE PATHWAY WITH NON-UNIFORM THERMAL CONDUCTIVITY FOR COOLING A HEAT GENERATING MEDIUM CONSIDERING THE THERMAL CONTACT RESISTANCE

E. X. Barreto

C. C. Beckel

L. A. O. Rocha

P. S. Schneider

ducaxb@hotmail.com

cassiabeckel@gmail.com

laorocha@gmail.com

pss@mecanica.ufrgs.br

Department of Mechanical Engineering, Federal University of Rio Grande do Sul

Rua Sarmento Leite, 425, 90050-170, Porto Alegre, RS, Brazil

E. D. Santos

L. A. Isoldi

elizaldosantos@furg.br

Liercioisoldi@furg.br

School of Engineering, Federal University of Rio Grande

Av. Itália km 8, 96201-900, Rio Grande, RS, Brazil

Abstract. *This numerical study applies the Constructal Design method to obtain the configuration that provides the easier access to the heat flowing through a T-shaped conductive pathway, with two different thermal conductivities, which is placed in a volumetric medium with low thermal conductivity and heat-generating. In this context, a third material located between the conductive pathway and the heat-generating medium has the function of thermal contact resistance. The objective function is to minimize the maximum temperature excess over the entire system (materials with high and low thermal conductivity and thermal contact resistance). Here, the heat conduction equation is solved using a numerical code based on finite elements approach, more specifically using the PDEtool in MATLAB environment. The total volume is fixed as well as the volume of the high thermal conductivity material and the amount of material that represents the thermal contact resistance. The configuration was optimized by varying the area fraction (ϕ_1), the lengths (L_1/L_0) and widths (D_1/D_0) of the two branches forming the "T", keeping fixed the aspect ratio of the area of the conductive material, ϕ, with respect to the total area of the body (A).*

Keywords: *Constructal Design, thermal contact resistance, heat transfer.*

1 INTRODUCTION

Cooling methods by insertion of pathways with high thermal conductive materials into heat-generating bodies have been widely used (Ledezma et al., 1997; Rocha et al., 2006; Boichot et al., 2009; Lorenzini et al., 2013) since Bejan's proposal in Bejan (1997) parallel to the rise of Constructal Law of Design and Evolution in Nature (Bejan et al., 2008; Bejan et al., 2012). However, all of these approaches assumes and ideal situation where the high conductive material performs a perfect thermal contact with the heat-generating medium, so, no temperature drop is considered in the interfaces. However, perfect thermal contact doesn't occur in nature due to imperfections in the interface of solids, roughness and flatness between the contact surfaces of the solids.

Commonly the imperfections in the contact surfaces of the solids make the contact area smaller than the nominal area of the surfaces. The voids at the interface are normally filled by air and in some cases special fluids are inserted in the interface aiming to improve the heat conduction through the solids. All the imperfections mentioned results in a thermal contact resistance, R_c'', at the interface of two solids placed in contact (Çengel, 2012). The thermal contact resistance has also been largely studied in the literature (Bahrami et al., 2004a; Goodarzi, et al., 2014; Bejan et al., 1993; Ghalambor et al., 2013).

In order to discover the configurations that most facilitates the access to the heat flow currents, Constructal Design is applied (Biserni et al., 2007; Lorenzini et al., 2006). This method applies the objective and constraints principle to find the best configuration in a deterministically way.

Here, Constructal Design is applied in a numerical work to study a system composed of a heat-generating medium and a T-shaped conductive pathway with different thermal conductivities on which the heat generated flows out through a heat sink. In all this analysis the thermal contact resistance was taken into account being compared with the results for an ideal situation, i.e., for the case of perfect thermal coupling.

2 MATHEMATICAL MODEL

Consider the body shown in Fig. 1. The configuration is two dimensional with the third dimension (W) sufficiently long compared with the height (H) and the length (L) of total volume. The vertical branch of the "T" has a thermal conductivity k_{p1} and the horizontal branch has a thermal conductivity k_{p2}. Both branches inserted in a body with lower thermal conductivity, k, and separated by a layer with high thermal resistance equivalent to the thermal contact resistance, k_L. The solid body generates heat uniformly by a volumetric rate q''' (W/m^3). The external surfaces are insulated and the generated heat current ($q'''AW$) is removed by a heat sink with a constant temperature, T_{min}, located in the rim of the body.

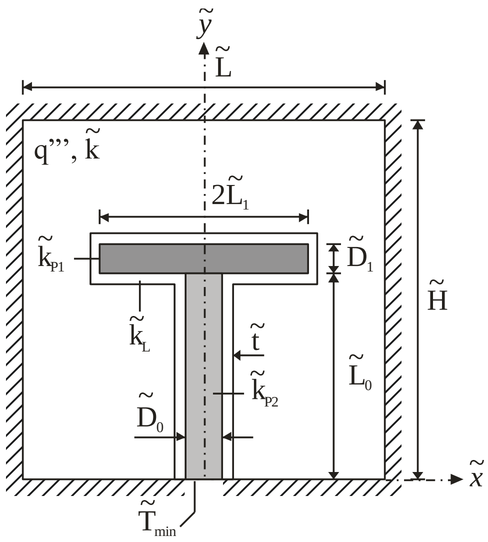

Figure 1. Conductive materials, k_{p1} and k_{p2}, with heat generation, whereas the thermal contact resistance.

The present work consists in calculate the maximal excess of dimensionless temperature $(T_{max} - T_{min})/(q'''A/k)$ and observe which geometry (L_1/L_0, D_0/L_0, ϕ_1) facilitates the heat removal. Here, special attention was given to the issue of thermal contact between the two elements with high thermal conductivity and the heat-generating volume. The thermal contact resistance between the two branches of the "*T*" are disregarded for the sake of simplicity.

The heat transfer through the two high conductive materials and the heat generating volume, both with cross-sectional area *A*, which is pressed against one another is the sum of heat transfer due to heat conduction through the points of contact and heat transfer by convection of air through the gaps, as can be seen in Fig. 2b.

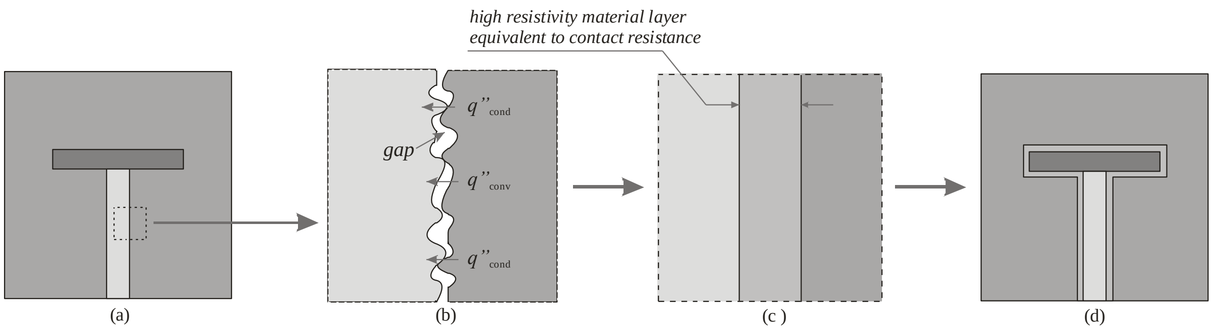

Figure 2. Heat conduction problem domain: (a) two elements of high conductivity and heat-generating body, (b) roughness of the surfaces, (c) layer of material between surfaces with resistivity equivalent to the thermal contact resistance, (d) configuration with third element used in the numerical simulation.

Equation (1) represents the total heat transfer shown in Fig. 2:

$$q'' = q''_{cond} + q''_{convec} \tag{1}$$

or similarly by Newton's law of cooling

$$q'' = h_c A \Delta T_{\text{int}} \tag{2}$$

where A is the apparent area of the interface, ΔT_{int} is the effective temperature difference at the interface. The heat transfer coefficient, h_c, is called thermal contact conductance and relates to the thermal contact resistance by

$$R_c'' = 1 / h_c \tag{3}$$

Thus, the thermal contact resistance is the inverse of thermal contact conductance and R_c'' represents the thermal contact resistance per unit area. The thermal contact resistance of the whole interface is then obtained dividing R_c'' by the total area. The value of R_c'' depends on many factors, such as the surface roughness, micro roughness, properties of solids involved, temperature, pressure which surfaces are submitted and the type of fluid interposed in the voids (gaps) of the interface. Experimental results show that R_c'' decreases with roughness decreasing and with pressure increasing on the interface.

Thus, in configurations involving multiple layers of high conductive materials such as metals, R_c'' can be very important and can interfere significantly on the overall thermal resistance of the system. In order to minimize R_c'' it is common to apply conductive liquids on interfaces with the purpose of replacing the air allocated through the gaps thus increasing the thermal conductance of the interface. This practice is commonly used in electronic components such as transistors connected to heat sinks, but there is a considerable uncertainty in literature about R_c'', so its use requires caution.

In this determining the maximum excess of dimensionless temperature of the overall system considering the thermal contact resistance, R_c'', it is convenient to estimate a layer of material interposed between the element of high thermal conductivity and the heat-generating volume having a thickness, t, and the thermal conductivity, k_L, whose thermal resistance is equal to the thermal contact resistance.

Aiming to determine the thickness, t, with a thermal resistance equivalent to the thermal contact resistance, it was used a one-dimensional approximation, as shown in Fig. 2c, also assumed a value of thermal conductance at the interface elements, $h_c = 2000$ $W/m^2 K$ and thermal conductivity $k_L = 10$ W/m K. Equation (4) determines the thickness, t, in dimensionless form where thermal resistance, R_c'', is obtained from Eq. (3). Thus,

$$\tilde{t} = \tilde{R}_c \tilde{k}_L \tag{4}$$

where $\tilde{t} = 0.005$, calculated from the arbitrated parameters for the proposed problem.

The present work is a heat transfer problem, considering steady state conditions and uniform heat generation, the thermal conductivity is assumed constant. The heat diffusion equation for the heat conductive body is described by

$$\frac{\partial^2 T}{\partial x^2} + \frac{\partial^2 T}{\partial y^2} + \frac{q'''}{k_p} = 0 \tag{5}$$

Equation (5) can be put in dimensionless form by using the dimensionless groups below:

$$\theta = \frac{T - T_{\min}}{q''' A / k_p} \quad (6)$$

$$\tilde{k}_p = \frac{k_p}{k} \quad (7)$$

$$\tilde{x}, \tilde{y}, \tilde{D}_0, \tilde{L}_0, \tilde{D}_1, \tilde{L}_1, \tilde{H}, \tilde{L} = \frac{x, y, D_0, L_0, D_1, L_1, H, L}{A^{1/2}} \quad (8)$$

where A in Eq. (6) is the area of the finite volume. The analysis that provides the excess of maximum temperature in function of the geometry in solving the heat diffusion equation with uniform heat generation along the region with low thermal conductivity, k. The dimensionless diffusion equation for the heat-generating body is described by:

$$\frac{\partial^2 \theta}{\partial \tilde{x}^2} + \frac{\partial^2 \theta}{\partial \tilde{y}^2} + 1 = 0 \quad (9)$$

Assuming that there is no heat generation in the material with high thermal conductivity, as well as in the layer whose thermal resistance is equivalent to the thermal contact resistance, the dimensionless heat conduction equation for these areas is given by:

$$\frac{\partial^2 \theta}{\partial \tilde{x}^2} + \frac{\partial^2 \theta}{\partial \tilde{y}^2} = 0 \quad (10)$$

The excess of maximum dimensionless temperature, $\theta_{\max}$, is defined as:

$$\theta_{\max} = \frac{T_{\max} - T_{\min}}{q''' A / k_p} \quad (11)$$

where k_p is the thermal conductivity between the conductive material and the environment. Evaluating the thermal resistance, Eqs. (9) and (10) are solved using boundary conditions considering the whole body as insulated except in the region where is located the heat sink $(-\tilde{D}_0 / 2 \leq \tilde{x} \leq \tilde{D}_0 / 2; \tilde{y} = 0)$ with temperature, $T_{\min}$. The boundary condition is given by a constant temperature:

$$\theta_0 = 0 \quad (12)$$

Once equations are defined, the next step is to reach the optimization, i.e., minimize the thermal resistance given by Eq. (11) when the total area and the thickness of the material that represents the thermal contact resistance are constant. According to the view of Constructal Design, the search may be subjected to two constraints area. The constraint of the total area,

$$A = HL \quad (13)$$

or described in dimensionless terms

$$\tilde{H}\tilde{L} = 1 \quad (14)$$

The area occupied by the high thermal conductivity material is given by:

$$A_p = A_{p1} + A_{p2} \quad (15)$$

where A_{p1} and A_{p2} are the two branches areas of the T-shaped high conductive pathway. Dividing Eq. (15) by the total area yields

$$\phi = \phi_1 + \phi_2 \tag{16}$$

In the optimization of this problem, it was assigned the value of H/L = 1 and ϕ = 0.1. Hence, it takes four dimensions that represent the problem domain: L_0, D_0, L_1 and D_1. Thus, two dimensionless parameters are chosen, L_1/L_0, D_0/L_0 and ϕ_1, as the degrees of freedom for varying the geometry that provides the lower thermal resistance. Using some algebra over Eq. (16) the following set of equations is obtained:

$$\tilde{L}_0 = \sqrt{(\phi - \phi_1)/(D_0/L_0)} \tag{17}$$

$$\tilde{D}_0 = \tilde{L}_0 (D_0/L_0) \tag{18}$$

$$\tilde{D}_1 = \left(\phi - \tilde{D}_0\tilde{L}_0\right)/\left[2\tilde{L}_0 (L_1/L_0)\right] \tag{19}$$

$$\tilde{L}_1 = \phi_1 / \left(2\tilde{D}_1\right) \tag{20}$$

Thus, with the equations above, it is possible to vary computationally the dimensionless parameters and, therefore, checking the geometry that facilitates – the heat flow out of the elementary volume. Then, for each degree of freedom is possible to find an optimum relation and the corresponding value $(\theta_{max})_m$, as the simulations are performed. Varying simultaneously two degrees of freedom is found a doubly optimum configuration $(\theta_{max})_{mm}$. Therefore, it is possible to generate configurations so many times optimized as the number of degrees of freedom simulated.

In the next section is performed a series of simulations varying the parameters L_1/L_0, D_0/L_0 and ϕ_1, in order to obtain the optimum geometry for each degree of freedom analyzed. In this context, the *root mean square* – RMS was used as a parameter of comparison of both models: the model with the presence of thermal contact resistance and the model where it was considered a perfect thermal coupling,

$$RMS = \sqrt{\frac{1}{n}\sum_{1}^{n}\left(\frac{x_i - x_r}{x_r}\right)^2} \times 100 \tag{21}$$

where the subscripts "*i*" and "*r*" refers to the configurations of ideal thermal contact and the one with thermal contact resistance.

3 NUMERICAL MODEL

The method was initially developed for a configuration with a T-shaped pathway. The function defined by Eq. (11) can be determined by the numerical solution of heat conduction given by Eqs. (9) and (10) for the temperature field at each assumed configuration, depending on the selected degree of freedom. The mesh used was determined by successive refinements, increasing the number of elements until the criterion $\left|\left(\theta_{max}^{j} - \theta_{max}^{j+1}\right)/\theta_{max}^{j}\right| \le 5\times10^{-4}$ is satisfied, where θ_{max}^{j} represents the maximum excess of dimensionless temperature calculated using the current mesh size, θ_{max}^{j+1} represents the maximum excess of dimensionless temperature using the following mesh, where the number of elements has been increased four times. The numerical solution of heat conduction equation was obtained with the implementation of a finite element code based on triangular elements developed in MATLAB environment. The parameters used in the simulations were: $\phi = 0.1$, $\tilde{k}_{p1} = 100$, $\tilde{k}_{p2} = 50$, $\tilde{k}_L = 0.05$ and $\tilde{k} = 1$. The geometry has been optimized considering its degrees of freedom and the results were compared with values obtained for an ideal situation, i.e., for a perfect thermal coupling situation. Tables 1 and 2 show the tests performed to obtain the mesh independence considering the case with thermal contact resistance and the case with perfect thermal coupling.

Table 1. Refinement of the mesh to obtain independent results of the number of elements, to ϕ_1 = 0.07, $(D_0/L_0)_o$ = 0.075 and $(L_1/L_0)_{oo}$ = 0.776 considering the thermal contact resistance

Number of nodes	Number of triangular elements	θ^{j}_{max}	$\theta^{j+1`}_{max}$	$\left|\left(\theta^{j}_{max} - \theta^{j+1}_{max}\right)/\,\theta^{j}_{max}\right| \leq 5\times10^{-4}$
5906	11669	0.170818	0.170619	1.17×10^{-3}
23480	46676	0.170619	0.170544	4.36×10^{-4}
93635	186704	0.170544	-	-

Table 2. Refinement of the mesh to obtain independent results of the number of elements, to ϕ_1 = 0.07, $(D_0/L_0)_o$ = 0.075 and $(L_1/L_0)_{oo}$ = 0.704 considering perfect thermal coupling

Number of nodes	Number of triangular elements	θ^{j}_{max}	$\theta^{j+1`}_{max}$	$\left|\left(\theta^{j}_{max} - \theta^{j+1}_{max}\right)/\,\theta^{j}_{max}\right| \leq 5\times10^{-4}$
235	419	0.135976	0.136468	3.62×10^{-3}
888	1676	0.136468	0.136639	1.26×10^{-3}
3451	6704	0.136639	0.136703	4.62×10^{-4}
13605	26816	0.136703	-	-

The ideal mesh, considering the proposed criterion mesh independence, consists of 46676 triangular elements for the case with contact resistance and 6704 triangular elements for the case with perfect thermal coupling.

4 RESULTS

4.1 Once optimized geometry

The numerical work consisted of determining the temperature field in a large number of configurations of the type shown in Fig. 1. In a first moment it was verified the maximum excess of dimensionless temperature of the solid body considering a range of values of L_1/L_0. It was chosen a configuration set as follows: ϕ_1 = 0.07, D_0/L_0 = 0.06 and L_1/L_0 varying from 0.2 until 0.7. Figure 3 covers this first analysis considering both models: the presence of the thermal contact resistance and the situation when it was assumed perfect thermal contact.

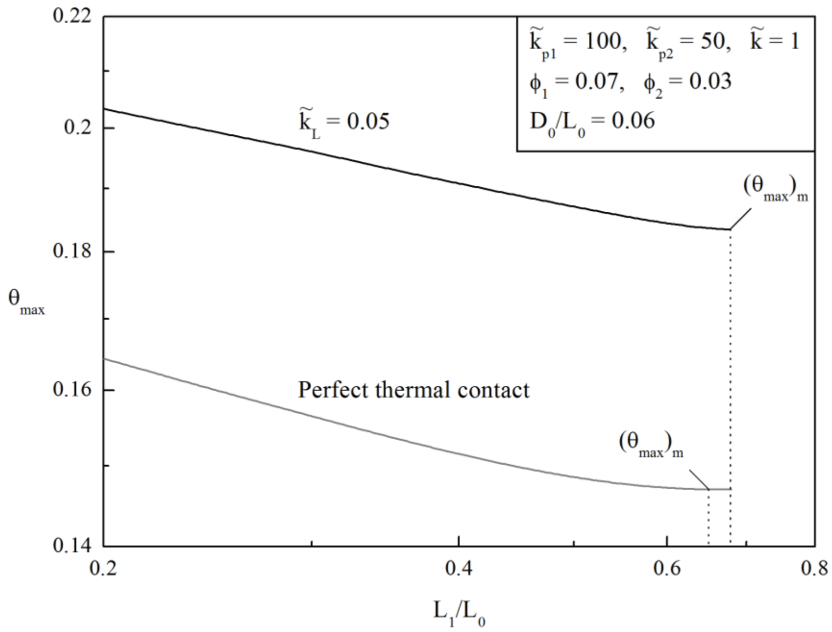

Figure 3. Maximum dimensionless excess of temperature, θ_{max}, for a range of L_1/L_0 considering perfect thermal contact and k_L = 0.05 for the case of the thermal contact resistance.

The optimization for a single degree of freedom as shown in Fig. 3 seems to follow the same behavior for both models: as the horizontal branch of the "*T*" approaches the wall (high values of L_1/L_0) the maximum dimensionless temperature assumes lower values. Indeed, the minimal values calculated for the maximum dimensionless temperature in both models were $(\theta_{max})_m$ = 0.1469 considering perfect thermal coupling and $(\theta_{max})_m$ = 0.1834 in the presence of the thermal contact resistance. The curve of thermal contact resistance in Fig. 3 seems to be almost equal to the perfect thermal coupling curve and plotted above from it. The temperature fluctuations between both curves were 20.17% and the fluctuation between the minimal values for the maximum dimensionless temperature of both models was 19.87%. Figure 4 presents a visualization of the two best configurations in this first analysis.

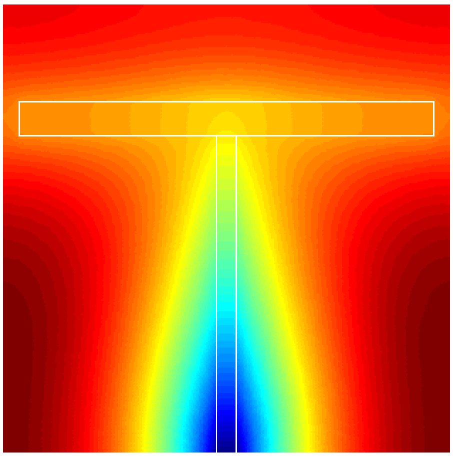

$(\theta_{max})_m$ = 0.1469
$(L_1/L_0)_o$ = 0.65
(a)

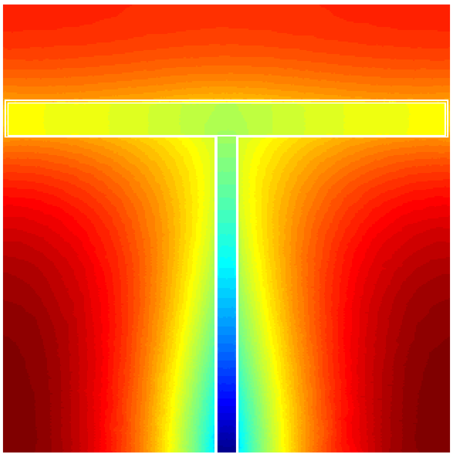

$(\theta_{max})_m$ = 0.1834
$(L_1/L_0)_o$ = 0.688
(b)

Figure 4. Optimized geometries for ϕ_1 = 0.07 and D_0/L_0 = 0.06: (a) model considering perfect thermal contact, (b) model including the thermal contact resistance.

4.2 Twice optimized geometry

The next analysis account to the simultaneous optimization of two degrees of freedom. This time, geometry was doubly optimized with respect to the ratios L_1/L_0 and D_0/L_0. The area fractions ϕ_1 and ϕ_2 remained the same values used in the first optimization as well as the other thermal properties. The same treatment given in section 4.1 was performed not for a single value of D_0/L_0 but for a range of values. Figures 5 and 6 show the doubly optimization analysis when D_0/L_0 ranged from 0.05 to 0.1

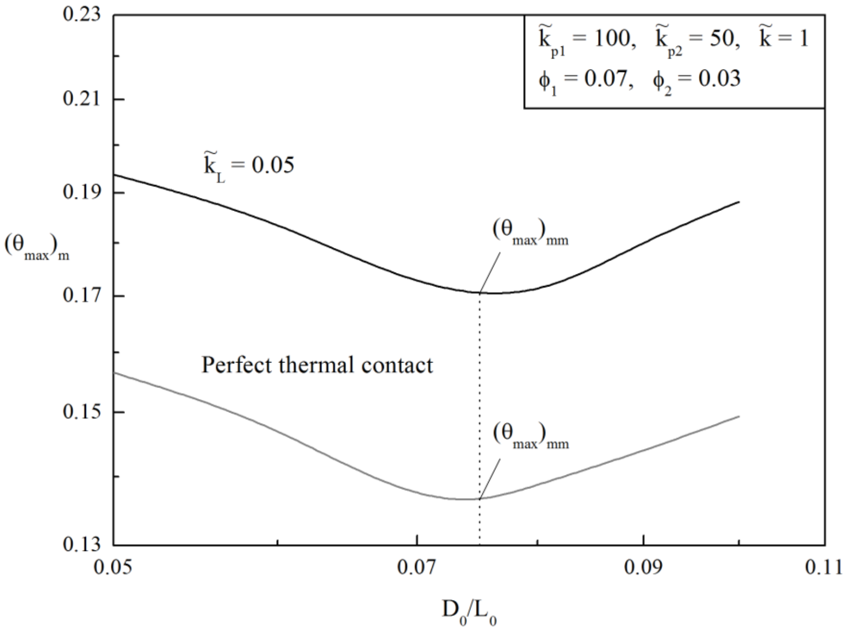

Figure 5. Curves of $(\theta_{max})_m$ and doubly minimized dimensionless temperature $(\theta_{max})_{mm}$, for fixed values of (H/L) and (ϕ_1) for a range of values of (L_1/L_0) and (D_0/L_0), considering simulations with and without contact resistance.

The analysis of Fig. 5 shows the curves of $(\theta_{max})_m$ for both models have the same profile being the thermal contact resistance curve plotted above the curve of perfect thermal coupling. The fluctuations between both curves ranged from 19.17% when D_0/L_0 = 0.05 until 20.62% when D_0/L_0 = 0.1. The RMS values obtained for both curves was 19.77%. The minimized excess of dimensionless temperature was $(\theta_{max})_{mm}$ = 0.1367 for the ideal situation and $(\theta_{max})_{mm}$ = 0.1706 for the case of thermal contact resistance, both temperatures were obtained for a ratio D_0/L_0 = 0.075. These numbers show the influence of thermal contact resistance concerning the rise of maximal excess of dimensionless temperature when this resistance was considered in numerical simulations. However the fluctuations of temperature between both models were almost equal concerning all the range of D_0/L_0 considered.

Similar analysis is performed in Fig. 6, when it was compared the variation of L_1/L_0 with the increasing of D_0/L_0 ratio in both models.

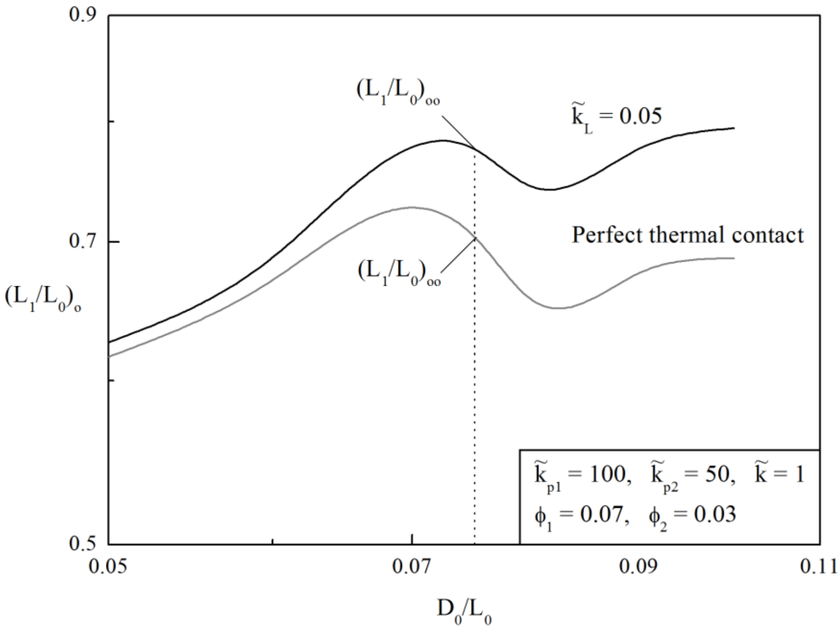

Figure 6. Curves of $(L_1/L_0)_o$ and doubly minimized dimensionless ratio $(L_1/L_0)_{oo}$, for fixed values of (H/L) and (ϕ_1) for a range of values of (D_0/L_0), considering simulations with and without contact resistance.

Here is noteworthy the influence of D_0/L_0 concerning fluctuations between the curves of $(L_1/L_0)_o$ for both models. Fluctuations of $(L_1/L_0)_o$ are smaller for small values of D_0/L_0, about 1.6% for $D_0/L_0 = 0.05$ and become higher with the increasing of D_0/L_0 achieving 13.48% for $D_0/L_0 = 0.1$. The RMS calculated over all the D_0/L_0 interval is 9.85%. Figure 5 has shown the twice minimized excess of dimensionless temperature for both models where the optimum ratio $(D_0/L_0)_o$ found was 0.075, the twiced optimized ratio $(L_1/L_0)_{oo}$ found for models with and without contact resistance was $(L_1/L_0)_{oo} = 0.776$ and $(L_1/L_0)_{oo} = 0.704$.

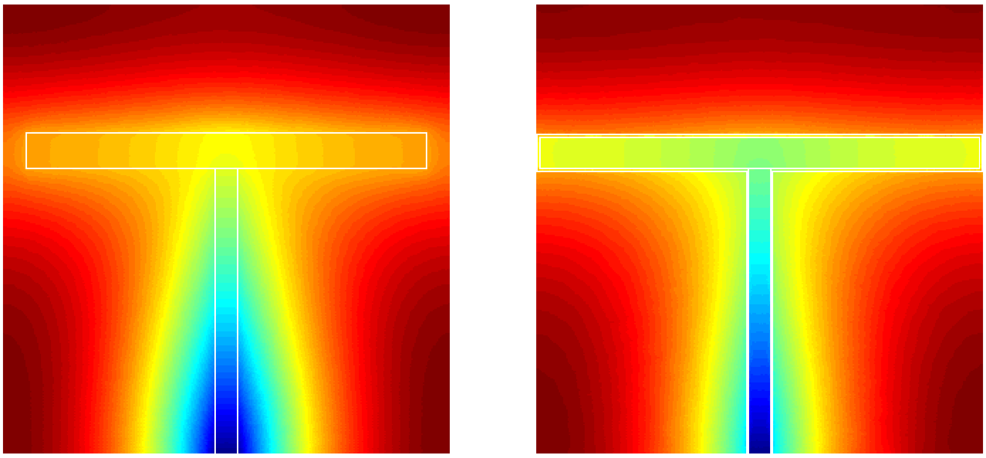

$(\theta_{max})_{mm} = 0.1367$
$(L_1/L_0)_{oo} = 0.704$
(a)

$(\theta_{max})_{mm} = 0.1706$
$(L_1/L_0)_{oo} = 0.776$
(b)

Figure 7. Doubly optimized geometries for $\phi_1 = 0.07$ and $(D_0/L_0)_o = 0.075$: (a) model considering perfect thermal contact, (b) model including the thermal contact resistance.

Figures 5 and 6 have shown the variation of D_0/L_0 has little importance in the variation of dimensionless temperature fluctuations but has significant influence in the variations of (L_1/L_0) fluctuations considering the model with perfect thermal coupling and the case with thermal contact resistance. Figure 7 presents a visual analysis of the doubly optimized geometries.

4.3 Three times optimized geometry

The last analysis of the geometry is remarkable to consider a total optimization of each degree of freedom of the problem. All the procedures achieved in the past sections for a fixed value of ϕ_1 (it was considered ϕ_1 = 0.07) are performed here for a range of ϕ_1 from 0.01 until 0.09. The result is a geometry three times optimized considering three degrees of freedom, i.e., an optimized geometry with respect to (ϕ_1), (L_1/L_0) and (D_0/L_0).

In the optimization process it was considered for each value of ϕ_1 a total of 6 simulations of the ratio (D_0/L_0) and 10 simulations of (L_1/L_0) for each value of (D_0/L_0) performing 60 simulations. As ϕ_1 has assumed 9 values from 0.01 to 0.09 it completes a total of 540 simulations.The numerical results show that the optimized geometry of the pathway tends to present a slender horizontal branch, i.e., the optimization process follows small values of ϕ_1 due to this is the area fraction of the smaller thermal conductivity of the pathway (k_{p1} = 50), so, for a better heat transfer it is desirable to have a bigger area fraction (ϕ_2) with a higher thermal conductivity (k_{p2} = 100). Figures 8 and 9 show the curves of $(\theta_{max})_{mm}$ and $(L_0/L_0)_{oo}$ obtained with the variation of ϕ_1.

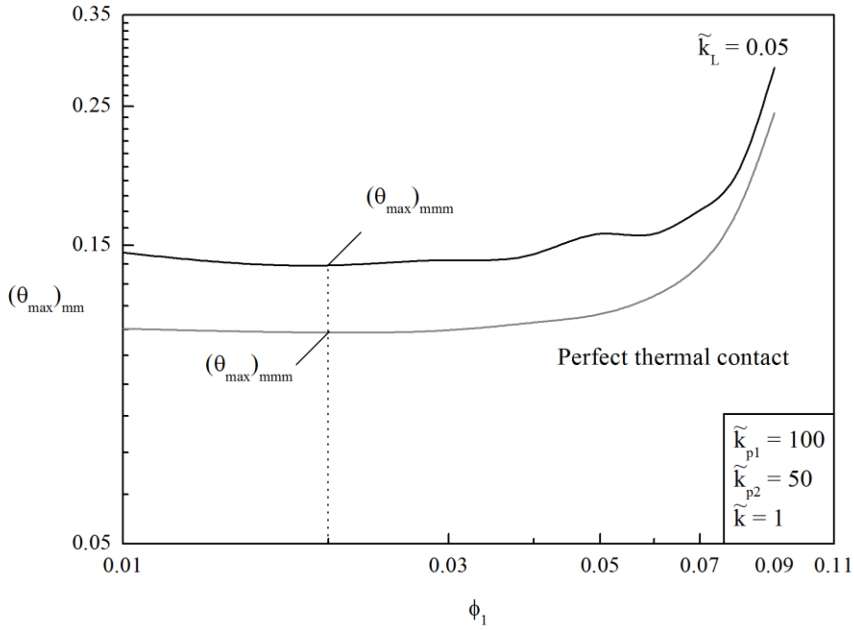

Figure 8. Curves of $(\theta_{max})_{mm}$ and three times minimized dimensionless temperature $(\theta_{max})_{mmm}$, for fixed value of (H/L) and a range of values of (ϕ_1), considering simulations with and without contact resistance.

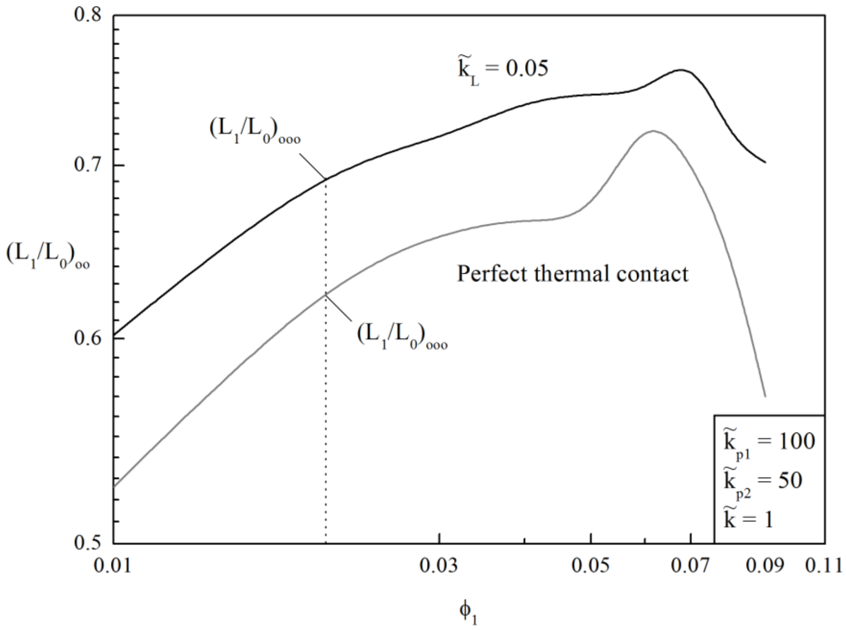

Figure 9. Curves of (L_1/L_0)$_{oo}$ and three times optimized ratio (L_1/L_0)$_{ooo}$, for fixed value of (H/L) and a range of values of (ϕ_1), considering simulations with and without contact resistance.

As shown in Figs. 8 and 9, the optimal value of ϕ_1 found was $(\phi_1)_o$= 0.02 for both models, i.e., with and without thermal contact resistance. The minimal excess of dimensionless temperature found in the numerical approximation was $(\theta_{max})_{mmm}$ = 0.1082 for the ideal situation and $(\theta_{max})_{mmm}$ = 0.1392 for the case of thermal contact resistance, then, presenting a variation of 22.22% between both values. The presence of the thermal contact resistance has influence in the determination of $(L_1/L_0)_{ooo}$, as seen in Fig. 9. Both models have presented fluctuations of 9.89% between $(L_1/L_0)_{ooo}$ of both models being $(L_1/L_0)_{ooo}$ = 0.629 for the ideal situation and $(L_1/L_0)_{ooo}$ = 0.698 for the case of thermal contact resistance.

A final analysis is presented in Figs. 10 and 11, where curves of $(\theta_{max})_{mm}$ and $(L_1/L_0)_{oo}$ of both models is presented with respect to $(D_0/L_0)_o$ using the optimal the already calculated optimal $(\phi_1)_o$= 0.02.

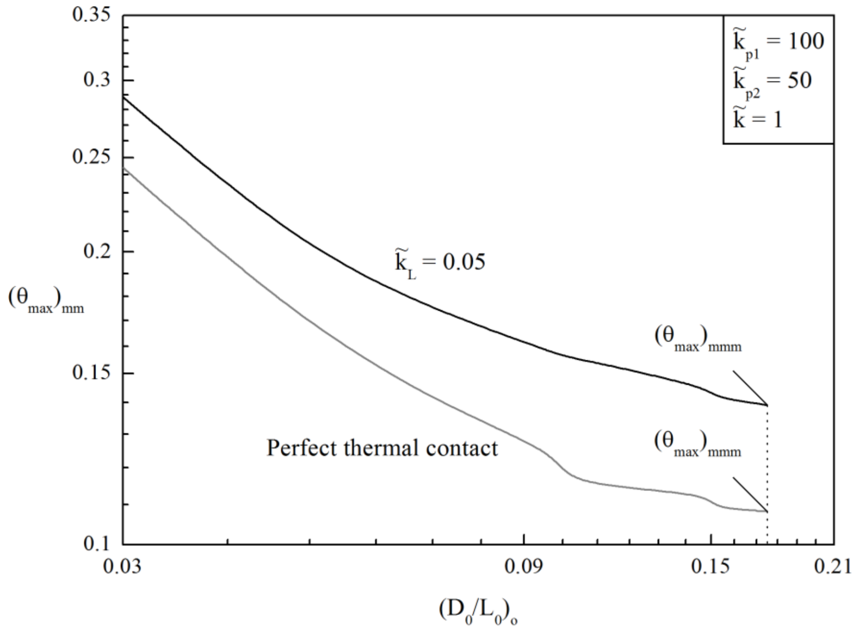

Figure 10. Curves of $(\theta_{max})_{mm}$ and three times minimized dimensionless temperature $(\theta_{max})_{mmm}$, for fixed value of (H/L) and a range of values of $(D_0/L_0)_o$, considering simulations with and without contact resistance.

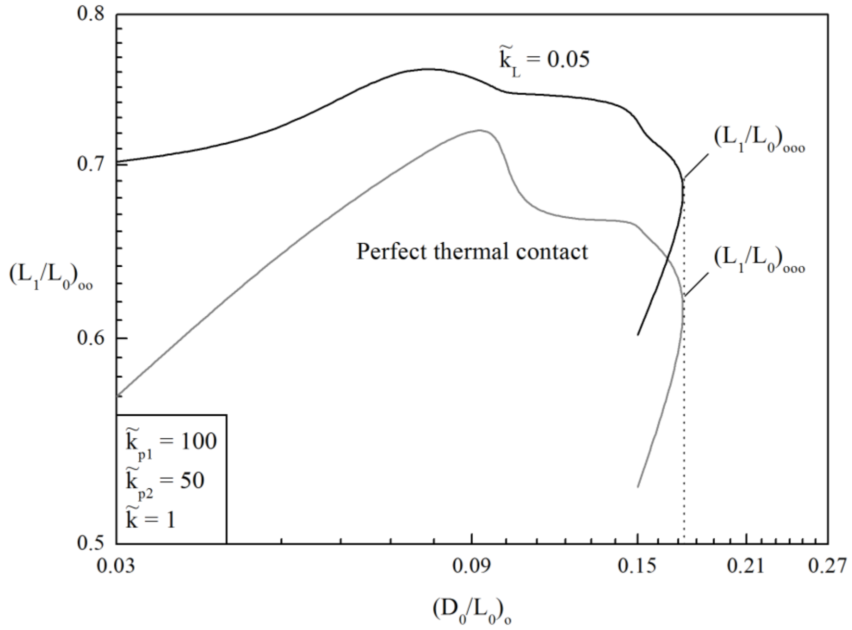

Figure 11. Curves of $(L_1/L_0)_{oo}$ and three times optimized ratio $(L_1/L_0)_{ooo}$, for fixed value of (H/L) and a range of values of $(D_0/L_0)_o$, considering simulations with and without contact resistance.

The optimum geometry was achieved for higher values of $(D_0/L_0)_o$. In both cases the optimum value of $(D_0/L_0)_o$ was $(D_0/L_0)_{oo}$ = 0.175 that shows the optimum geometry tends to touch the upper wall of the volume in order to achieve a better temperature distribution. The three times optimized geometry for both models are visualized in the Fig. 12 below.

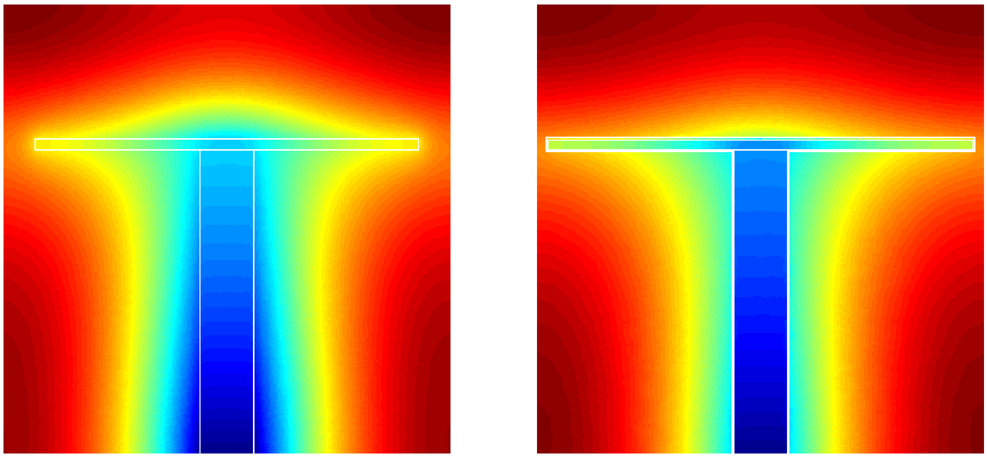

$(\theta_{max})_{mmm} = 0.1082$
$(L_1/L_0)_{ooo} = 0.629$
(a)

$(\theta_{max})_{mmm} = 0.1392$
$(L_1/L_0)_{ooo} = 0.698$
(b)

Figure 12. Three times optimized geometries for $(\phi_1)_o = 0.02$ and $(D_0/L_0)_{oo} = 0.175$: (a) model considering perfect thermal contact, (b) model including the thermal contact resistance.

5 CONCLUSIONS

A numerical study was conducted aiming to achieve an optimized geometry of a T-shaped pathway for cooling a heat-generating body considering both: the presence or not of thermal contact resistance. The optimized process account with the optimization of three degrees of freedom: ϕ_1, L_1/L_0 and D_0/L_0 and the process was divided in the optimization of a single degree of freedom, following of the simultaneous optimization of two degrees of freedom and finally the three degrees of freedom together.

In this process it was noted that the presence of the thermal contact resistance has direct influence in the increasing of the minimal excess of dimensionless temperature of the body, with fluctuations equal to 21.46% in the RMS values between both models.

Even though the optimum $(\phi_1)_o$ and $(D_0/L_0)_{oo}$ has no difference between the models with and without thermal resistance, fluctuations close to 10% were verified with respect to the ratio $(L_1/L_0)_{oo}$ of both models.

It is worth to notice that the performance of the configurations is very similar in the range $0.01 < \phi_1 < 0.04$ according to Fig. 8. Therefore, to save high conductivity material, i.e. to reduce costs, it is recommended to use $\phi_{1,o} = 0.04$ and its corresponding optimal geometric ratios.

Thus, the differences of temperatures added to the differences between the optimized ratio $(L_1/L_0)_{oo}$ of both models are enough arguments that make the presence of thermal contact resistance an important issue to be considered in the optimization of thermal systems.

Acknowledgements

Elizaldo D. dos Santos, Liércio A. Isoldi, C. C. Beckel, Paulo S. Schneider and Luiz A. O. Rocha thank the sponsorship to CNPq, Brasília, DF, Brazil. E. X. Barreto acknowledges the financial support of Capes, Brasília, DF, Brazil.

REFERENCES

Bahrami, M., Culham, J. R., Yovanovich, M. M., Schneider, G. E., 2004a. Thermal Contact Resistance of Nonconforming Rough Surfaces, Part 1: Contac Mechanics Model, Journal Thermophys. Heat Transfer, 18(2) 209-217.

Bahrami, M., Culham, J. R., Yovanovich, M. M., Schneider, G. E., 2004b, Thermal Contact Resistance of Nonconforming Rough Surfaces, Part 2: Thermal Model, Journal Thermophys. Heat Transfer, 18(2) 218-227.

Bejan, A., Morega, A. M., 1993. Thermal contact resistance between two flat surfaces that squeeze a film of lubrificant, J. Heat Transfer, 115 763-767.

Bejan, A., 1997. Constructal-theory network of conducting paths for cooling a heat generating volume, Int. J. Heat Mass Transf. 40 (4) 799-816.

Bejan, A., Lorente, S., 2008. Design with Constructal Theory, Wiley, New Jersey.

Bejan, A., Zane, J. P., 2012. Design in Nature: How the Constructal Law Governs Evolution in Biology, Physics, Technology, and Social Organization, Random House LLC, New York.

Biserni, C., Rocha, L. A. O., Stanescu, G., Lorenzini, G. 2007. Constructal H-shaped cavities according to Bejan's theory, Int. J. Heat Mass Transf. 50 2132 – 2138.

Boichot, R., Luo, L., Fan, Y., 2009. Tree-network structure generation for heat conduction by cellular automaton, Energy Convers. Manage. 50 376–386.

Çengel, Y. A., Ghajar, A. J., 2012. Heat & Mass Transfer: A Practical Approach, MC Graw-Hill Education , New York.

Cui, T., Li, Q., Xuan, Y., Zhang, P. 2014. Multiscale simulation of termal contact resistance in electronic packaging, Int. J. Therm. Sci. 83 16-24.

Da Silva, A.K., Vasile, C., Bejan, A., 2004. Disc cooled with high-conductivity inserts that extend inward from the perimeter, Int. J. Heat Mass Transf. 47 4257–4263.

Dirker, J., Meyer, J. P., 2009a. Heat removal from power electronics in two direction sets using embedded solid state cooling layers – a proposed non-numerical calculation method, Heat Transfer Eng. 30 (6) 452-465.

Dirker J., and Meyer J.P., 2009b. Thermal characterization of embedded heat spreading layers in rectangular heat-generating electronic modules, Int. J. Heat Mass Transf. 52 1374-1384.

Ghalambor, S., Agonafer, D., Haji-Sheikh, A. 2013. Analytical Thermal Solution to a Nonuniformly Powered Stack Package with Contact Resistance, J. Heat Transfer, 135 111015-1 (9 pages).

Ghodoossi, L. Egrican, N., 2004. Conductive cooling of triangular shaped electronics using constructal theory, Energy Convers. Manage. 45 811–828.

Goodarzi, K., Ramezani, S. R., Hajati, S., 2014. Reducing thermal contact resistance using nanocoating, Appl. Therm. Eng. 70 641-646.

Hajmohammadi, M. R., Alizadeh Abianeh, V., Moezzinajafabadi, M., Daneshi, M., 2013. Fork-shaped highly conductive pathways for maximum cooling in a heat generating piece. Appl. Therm. Eng. 61 228–35. doi:10.1016/j.applthermaleng.2013.08.001.

Hajmohammadi, M. R., Shariatzadeh, O. J., 2014. Phi and Psi shaped conductive routes for improved cooling in a heat generating piece. Int. J. Therm. Sci. 77 66–74.

Horbach, C. S., Dos Santos, E. D., Isoldi, L. A., Rocha, L. A. O., 2014. Constructal design of Y-shaped pathways for cooling a heat-generating body, Defect Diffus. Forum 348 (1) 245-260.

Kuddusi, L., Denton, J. C., 2007. Analytical solution for heat conduction in composite slabs and its implementation in constructal solution for cooling of electronics, Energy Convers. Manage. 48 1089-1105.

Ledezma, G. A., Bejan, A., Errera, M. R., 1997. Constructal tree networks for heat transfer, J. Appl. Phys. 82 (1) 89–100.

Li, Q., Steven, G. P., Xie, Y. M., Querin, O. M., 2004. Evolutionary topology optimization for temperature reduction of heat conducting fields, Int. J. Heat Mass Transf. 47 (23) 5071–5083.

Lingen, Z. C., Fengrui, S., 2007. Optimization of constructal volume-point conduction with variable cross section conducting path, Energy Convers. Manage. 48 (1) 106-111.

Lorenzini, G., Rocha, L. A. O. 2006. Constructal Design of Y-Shaped Assembly of Fins, Int. J. Heat Mass Transf. 49 4552-4557.

Lorenzini, G., Biserni, C., Rocha, L. A. O., 2013a. Constructal design of X-shaped conductive pathways for cooling a heat-generating body, Int. J. Heat Mass Transf. 58 513-520.

Lorenzini, G., Biserni, C., Rocha, L. A. O. 2013b. Constructal design of non-uniform X-shaped conductive pathways for cooling, Int. J. Thermal Sci. 71 140-147.

MATLAB, 2000. user's guide, version 6.0.088, release 12, The Mathworks Inc.

Rocha, L.A.O., Lorente, S., Bejan, A., 2002. Constructal design for cooling a disc-shaped area by conduction, Int. J. Heat Mass Transf. 45 1643-1652.

Rocha, L. A. O., Lorente, S., Bejan, A., 2006. Conduction tree networks with loops for cooling a heat generating volume, Int. J. Heat Mass Transf. 49 2626-2635.

Steven, G. P., Li, Q., Xie, Y. M., 2000. Evolutionary topology and shape design for general physical field problem, Comput. Mech. 26 (2) 129–139.